Nature Environment and Pollution Technology
An International Quarterly Scientific Journal

p-ISSN: 0972-6268
(Print copies up to 2016)
e-ISSN: 2395-3454

Vol. 21 | No. 3 | pp. 1073-1085 | 2022

Original Research Paper

https://doi.org/10.46488/NEPT.2022.v21i03.013

Open Access Journal

The Influence of Floodplain Vegetation Patches on Hydrodynamic Characteristics: A Case Study in the Old Course of Fuhe River

Da Li*, Zhonghua Yang*†, Junjie Zheng*, Fangping Liu and Gang Ge*****

*State Key Laboratory of Water Resources and Hydropower Engineering Science, Wuhan University, Wuhan 430072, China

**Jiangxi Irrigation Experiment Central Station, Nanchang 330031, China

***School of Life Science, Nanchang University, Nanchang 330031, China

†Corresponding author: Zhonghua Yang; yzh@whu.edu.cn

Nat. Env. & Poll. Tech.
Website: www.neptjournal.com

Received: 17-09-2021
Revised: 10-11-2021
Accepted: 20-11-2021

Key Words:
Fuhe river
Floodplain
Vegetation patches
Hydrodynamic characteristics
Equivalent Manning coefficient

ABSTRACT

As an important part of the river ecosystem, vegetation has a significant influence on hydrodynamic characteristics, water quality, river morphology, and ecological habitat. Combining vegetation survey with the verified numerical model, this study aims to analyze the impact of floodplain vegetation patches on hydrodynamic characteristics in the old course of Fuhe River under various combinations of incoming flow discharges, and flood diversion discharges, and changes in the land use type. The equivalent Manning coefficient was adopted to quantify the additional resistance induced by plants in the vegetation module of the numerical model. According to simulating results, vegetation patches would cause the water level to rise and velocity to decrease, which mainly affects the upstream of the old course of Fuhe River. And with the increase in incoming discharge, water level difference and velocity difference have an upward trend. It is also found that the resistance of *Zizania latifolia* to river flow is strongest followed by sugarcane, crops, and weeds because of the differences in vegetation characteristics. Furthermore, compared with existing vegetation conditions, converting farmland to *Zizania latifolia* and expanding farmland induce a moderate rise in water level upstream while the decreasing velocity happens in the area where land use type is changed. And there are areas where velocity increases located opposite to the velocity decreasing area because of the adjustment of cross-section velocity distribution caused by plants.

INTRODUCTION

In nature, aquatic plants are abundant in rivers and also have a significant influence on the river ecosystems by altering flow fields, stabilizing river beds, sheltering aquatic animals, and enhancing water quality. With the popularization of the concept of ecological rivers and river restoration, aquatic vegetation is introduced in the design of ecological rivers and restoration engineering projects. Therefore, more and more attention is paid to the vegetation impact on natural river ecosystems, which is helpful for better river management and protection.

Aquatic plants directly impact flow dynamics. First of all, compared with non-vegetated rivers, the existence of aquatic plants would induce additional flow resistance, which causes the flow velocity to slow down and the water level to rise. To quantify the obstruction of vegetation, the vegetation drag coefficient, C_D is introduced as an important parameter that is related to the vegetation characteristics and the flow conditions. In the previous studies, several predicting formulas C_D were proposed, which were systematically reviewed and summarized by Liu et al. (2020) and D'ippolito et al. (2021). And the profile of velocity distribution in vegetated channels is also affected by vegetation. Generally, the velocity in the emergent vegetation layer almost distributes uniformly while the velocity distribution profile is variable along the water depth in the submerged canopy layer. Therefore, to describe the key parameter in the submerged vegetation layer, different velocity models were proposed, such as the two-layer velocity model (Yang & Choi 2010) and the three-layer velocity model (Nepf 2012). Besides, bed shear stress (Etminan et al. 2018, Yang et al. 2015), Reynolds shear stress (Choi & Kang 2004, Dijkstra & Uittenbogaard 2010), the development of shear layer caused by vegetation (Ghisalberti & Nepf 2006), and other turbulent characteristics (Zhao et al. 2019) were focused on.

Heavily affected by the flow field, sediment transport in vegetated channels is also changed. In terms of sediment transport in vegetated rivers, previous research mainly concentrated on the initiated sediment motion (Cheng et al.

2020), bed-load transport rate (Yang & Nepf 2018), the distribution profile of suspended sediment concentration (SSC) (Huai et al. 2019, Li et al. 2020), the sediment erosion and deposition (Follett & Nepf 2018, Västilä & Järvelä 2018). Compared with non-vegetated channels, the critical flow velocity and the turbulent kinetic energy are supposed to be better indicators for predicting the initiated sediment motion and the bed-load transport rate, respectively (Tinoco & Coco 2016). In terms of the SSC distribution profile, recent studies mainly depend on three theories: the diffusion theory, the gravitational theory, and the random displacement model. As for the sediment erosion and deposition in vegetated channels, flume experiments found that sediment particles are usually scoured from the leading area of the vegetation region but deposited in the latter length of the vegetation area or behind the patch.

To simulate the interaction between the flow dynamics and vegetation, a lot of numerical models were proposed in the previous studies. In these numerical models, the widely adopted numerical methods are Boussinesp wave equations (Augustin et al. 2009, Huang et al. 2011), Navier-Stokes equations, and 2D shallow water equations (Bai et al. 2016, Wu & Marsooli 2012).

This study firstly introduces the vegetation module, which adopts the equivalent Manning coefficient to quantify vegetation resistance, into the hydrodynamic model. And based on the field vegetation investigation results, this paper aims to investigate how the vegetation patches on floodplains influence the flow dynamics in the old course of the Fuhe River by considering the combined effect of flood diversion and the changes in vegetation types, which is helpful to better river management and flood prevention.

MATERIALS AND METHODS

Hydrodynamic Module

This paper adopts the well-balanced two-dimensional shallow water equation which considers vegetation factors, wind stress, and Coriolis force. Its conservative form is described as:

$$\frac{\partial \mathbf{U}}{\partial t}+\frac{\partial \mathbf{F}}{\partial x}+\frac{\partial \mathbf{G}}{\partial y}=\mathbf{S}_b+\mathbf{S}_t+\mathbf{S}_f+\mathbf{S}_v \qquad \ldots(1)$$

where **U** is the vector of conserved variables; **F** and **G** are the vectors of fluxes along the x and y directions respectively; t represents time; x and y denote the Cartesian coordinates; $\mathbf{S}_b$ is the vector of slope source term; $\mathbf{S}_t$ is the vector of turbulence resistance source term; $\mathbf{S}_f$ is the vector of source term of river bed friction, and $\mathbf{S}_v$ is the vector of source term of additional resistance induced by vegetation. The vectors mentioned above are defined as:

$$\mathbf{U}=\begin{bmatrix}\eta\\ q_x\\ q_y\end{bmatrix},\ \mathbf{F}=\begin{bmatrix}q_x\\ q_x^2/h+\frac{1}{2}g\left(\eta^2-2\eta z_b\right)\\ q_y\end{bmatrix},\ \mathbf{G}=\begin{bmatrix}q_y\\ q_x\\ q_y^2/h+\frac{1}{2}g\left(\eta^2-2\eta z_b\right)\end{bmatrix}$$

$$\mathbf{S}_b=\begin{bmatrix}0\\ -g\eta\frac{\partial z_b}{\partial x}\\ -g\eta\frac{\partial z_b}{\partial y}\end{bmatrix},\ \mathbf{S}_f=\begin{bmatrix}0\\ -\frac{gn_b^2}{h^{1/3}}u\sqrt{u^2+v^2}\\ -\frac{gn_b^2}{h^{1/3}}v\sqrt{u^2+v^2}\end{bmatrix},\ \mathbf{S}_v=\begin{bmatrix}0\\ -\frac{F_{vx}}{\rho}\\ -\frac{F_{vy}}{\rho}\end{bmatrix} \qquad \ldots(2)$$

where g is the acceleration of gravity; h denotes water depth; z_b is river bed elevation; η denotes water level and $\eta = h + z_b$; u and v are velocity components in x and y directions, respectively; $q_x = hu$ and $q_y = hv$ represent the discharges per width in x and y directions; and n is Manning coefficient of the river bed.

In the shallow water equation, the depth-averaged turbulent shear stress is determined according to the Boussinesq assumption and it is written as:

$$\mathbf{S}_t=\begin{bmatrix}0\\ \frac{\partial\left(hT_{xx}\right)}{\partial x}+\frac{\partial\left(hT_{yx}\right)}{\partial y}\\ \frac{\partial\left(hT_{xy}\right)}{\partial x}+\frac{\partial\left(hT_{yy}\right)}{\partial y}\end{bmatrix},\ \begin{cases}T_{xx}=2\nu_t\frac{\partial u}{\partial x}\\ T_{xy}=T_{yx}=\nu_t\left(\frac{\partial u}{\partial y}+\frac{\partial v}{\partial x}\right)\\ T_{yy}=2\nu_t\frac{\partial v}{\partial y}\end{cases} \qquad \ldots(3)$$

where ν_t is eddy viscosity which can be quantified by the following equations:

$$\nu_t=0.5hu^*,\ u^*=\left[c_f\left(u^2+v^2\right)\right]^{1/2},\ c_f=gn_b^2/h^{1/3} \qquad \ldots(4)$$

Vegetation Module

Vegetation usually grows on the floodplain, inducing additional flow resistance. At present, plants can be divided into rigid and flexible vegetation according to rigidity. Rigid vegetation is usually treated as cylindrical piles while flexible vegetation cannot be treated as the same since it could be deflected by river flow. Thus, the mean deflected height is used as the characteristic height of flexible vegetation. To quantify the additional vegetation resistance, vegetation drag

force and equivalent Manning coefficient were proposed, respectively.

In terms of vegetation drag force, it is commonly described based on the drag coefficient (Whittaker et al. 2015):

$$\mathbf{F}_v = \frac{1}{2}\rho\lambda C_D C_a^{\psi/2} h \left|\mathbf{U}_C\right| \mathbf{U}_C \quad \ldots(5)$$

where ρ is water density; λ denotes the projected area of vegetation per unit volume of water in the direction of water flow; $\mathbf{U}_c$ is the mean velocity in the vegetation layer (Stone & Shen 2002); C_a is Cauchy number of flexible; ψ is the parameter representing the flexibility of vegetation, which ranges from -1 to 0. For rigid vegetation, the value of ψ is 0. C_D is related to flow velocity, vegetation characteristics, and fluid viscosity. Schlichting and Gersten (2017) proposed a method (Eq. (6)) to determine the drag coefficient based on the Reynolds number.

$$C_D = \begin{cases} 3.07e^{-0.168} & \mathrm{Re} = uD/\nu < 800 \\ 1.0 & 800 \le \mathrm{Re} < 8000 \\ 1.2 & 8000 \le \mathrm{Re} < 10^5 \end{cases} \quad \ldots(6)$$

Where Re is Reynolds number and D is the vegetation diameter. And due to differences in morphological characteristics of various types of vegetation, different empirical formulas to quantify the value C_D have been proposed (Etminan et al. 2017, Sonnenwald et al. 2019). However, in the shallow water mathematical model, the drag coefficient is often taken as a constant ranging from 0.8 to 1.5.

For the area in rivers covered with vegetation patches, the equivalent Manning coefficient is used to determine the combined resistance of river bed resistance and the additional resistance induced by vegetation. The combination of the source terms of resistance $\mathbf{S}_f$ and $\mathbf{S}_v$ in Eq. (1) could be written as:

$$\mathbf{S}_f + \mathbf{S}_v = \begin{bmatrix} 0 \\ -\dfrac{g\left(n_v^2 + n_b^2\right)}{h^{1/3}} u\sqrt{u^2+v^2} \\ -\dfrac{g\left(n_v^2 + n_b^2\right)}{h^{1/3}} v\sqrt{u^2+v^2} \end{bmatrix} = \begin{bmatrix} 0 \\ -\dfrac{g\bar{n}^2}{h^{1/3}} u\sqrt{u^2+v^2} \\ -\dfrac{g\bar{n}^2}{h^{1/3}} v\sqrt{u^2+v^2} \end{bmatrix} \quad \ldots(7)$$

Where n_v denotes the Manning coefficient quantifying the vegetation resistance and n_b is the Manning coefficient of river bed resistance. $\bar{n} = \sqrt{n_v^2 + n_b^2}$ is equivalent Manning coefficient in vegetation area. Based on the principle of equivalence, the equation to determine the equivalent Manning coefficient is proposed (Huai et al. 2012), which could be described as:

$$\bar{n} = \sqrt{(1-c)n_b^2 + \frac{2C_D\alpha_v\xi^2 c \min\left(h,\ h_v\right)h^{1/3}}{g\pi D}} \quad \ldots(8)$$

Where c is vegetation density and $c = c_v\min(h, h_v)/h$; c_v is the ratio of vegetation volume to water volume in the vegetation layer; α_v indicates shape factor whose value is usually 1.0 for cylindrical vegetation; ξ is a constant called velocity correction factor which is nearly 1.0; h_v is vegetation height.

In the vegetation module of a mathematical model, an equivalent Manning coefficient is adopted to represent the combined resistance of the vegetation patch. The equivalent Manning coefficient of each vegetation patch needs to be determined according to the water depth and vegetation characteristics (density, diameter and height) of each vegetation patch.

Numerical Scheme

Eq. (1) is spatially discretized by applying the cell-centered finite volume method based on the Godunov scheme, which can be described as:

$$\mathbf{U}_{i,j}^{m+1} = \mathbf{U}_{i,j}^{m} - \frac{\Delta t}{\Delta x_{i,j}}\left[\mathbf{F}_{i+\frac{1}{2},j} - \mathbf{F}_{i-\frac{1}{2},j}\right] - \frac{\Delta t}{\Delta y_{i,j}}\left[\mathbf{G}_{i,j+\frac{1}{2}} - \mathbf{G}_{i,j-\frac{1}{2}}\right] + \Delta t\mathbf{S}_{i,j} \quad \ldots(9)$$

Where m denotes time level; i and j represent cell indexes; Δt is time step; Δx and Δy are space steps in x and y directions, respectively; $\mathbf{F}_{i+\frac{1}{2},j}$, $\mathbf{F}_{i-\frac{1}{2},j}$, $\mathbf{G}_{i,j+\frac{1}{2}}$ and $\mathbf{G}_{i,j-\frac{1}{2}}$ are the vectors of fluxes in the east, west, north, and south interfaces respectively.

The cell boundary fluxes are calculated using the approximate Riemann solver of the HLLC format, which considers the influence of the medium wave (Toro et al. 1994). This study adopts the two-stage explicit Runge-Kutta scheme (Hou et al. 2013) to achieve a second-order temporal accuracy and update the conserved flow variables at a new time level. Besides, to obtain the second-order accuracy in space, the MUSCL scheme was chosen to linearly reconstruct the conserved flow variables in each cell. The numerical computation in this study was performed by our program which has proved the capability of the finite-volume Godunov-type scheme (Bai et al. 2016, Zhu et al. 2018).

Study Area and Field Investigation

As a tributary of Fuhe River, the old course of Fuhe River is located in Jiangxi Province, China, as shown in Fig. 1. The old course of Fuhe River starts from the flood diversion sluice of Jianjiang River and flows to Gangqian dam, with a total length of 18km approximately. The width of the river channel ranges from 100 to 800 meters. As a section of the West Main Canal of Ganfu Plain, the old course of Fuhe River is an important part of non-engineering measures of Fuhe River for flood control by holding the discharged water from the mainstream of Fuhe River. During the non-flood season, the incoming water is completely introduced by Jiaoshi Barrage Dam and flows into the old course of Fuhe River through West Main Canal. The entire river, especially the upper reaches, has a good ecosystem and is less affected by human activities.

The vegetation distribution in the old course of the Fuhe River was investigated in 2017, including vegetation species, location, density, height, and other characteristics. The main vegetation species and land use types are shown in Fig. 2. According to the field survey results, *Eichhornia crassipes* and *Zizania latifolia* are the absolute dominant species, accounting for approximately 51.80% and 54.27% of the survey plots, respectively. The biomass of the two dominant plants reaches the maximum level in September and then decreases from September to November. Based on the rigidity and submergence of vegetation, the distribution of vegetation species and land use types are simplified as shown in Fig. 3 to quantify the resistance coefficient of each zone easily. The study area is divided into 75 sub-areas in total. The vegetation species, water blocking structures, and basic parameters of each sub-area are listed in Table 1.

VALIDATION

A set of flume experiment data and a set of measured data from the old course of Fuhe River were adopted to verify the numerical model. The flume experiment conducted by Pasche and Rouvé (1985) is about overbank flow on floodplains covered with vegetation. The experiment was conducted in a tilting flume with a bottom slope of 0.0005 and a bottom Manning coefficient of 0.01. The flume is 25.5 m long and 1 m wide with a trapezoidal cross-section. Two vegetation densities were considered, 0.013 (Run M-1) and 0.025 (Run M-2), with the corresponding flow discharge of 0.0345 $m^3.s^{-1}$ and 0.0365 $m^3.s^{-1}$, respectively. The hydrological data measured in the old course of Fuhe River includes the in-

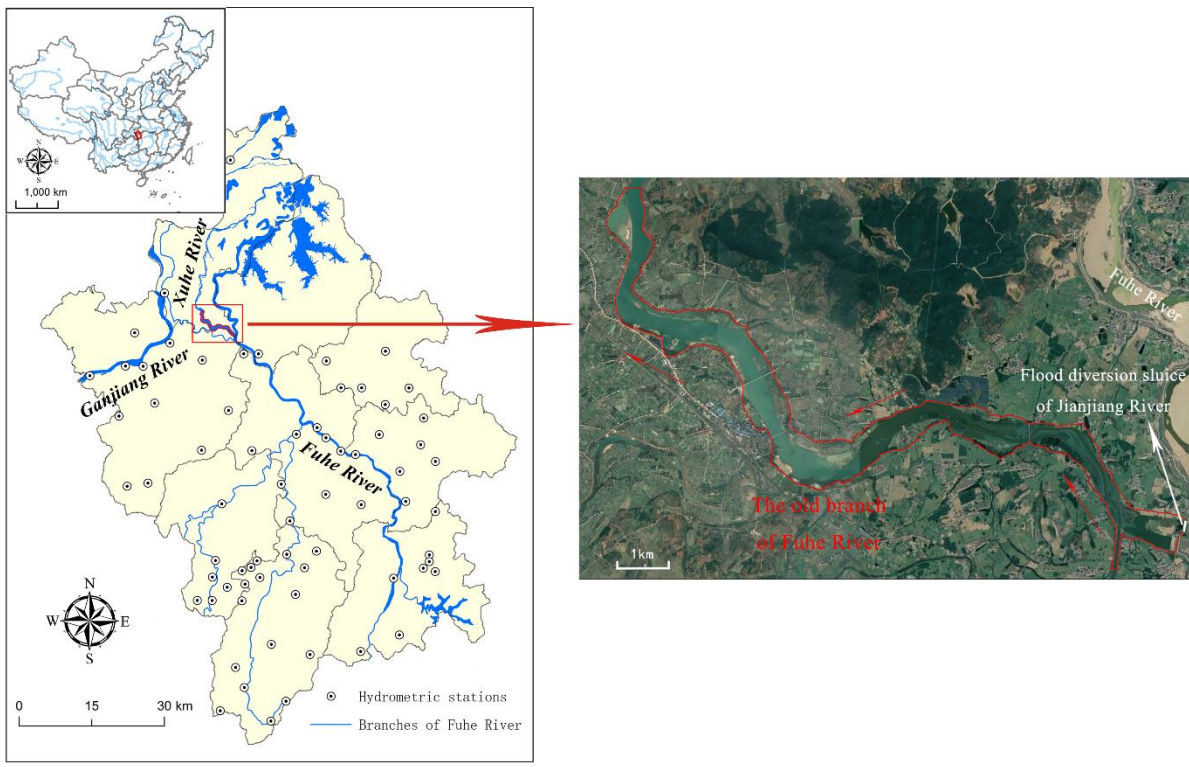

Fig. 1: Location of the old course of Fuhe River.

Table 1: Details of each sub-area.

Species	Area Number	Height [m]	Diameter [m]	Density
Weeds	1-3	0.12	0.0025	0.0108
	19	0.14	0.0021	0.0082
Sugarcane	4	2.20	0.0420	0.0130
Crops	5-13	0.21	0.0024	0.0100
Zizania latifolia	15	1.70	0.0087	0.0118
	16	1.74	0.0085	0.0121
	20	2.20	0.0150	0.0176
	22, 23, 25, 26, 30	1.75	0.0085	0.0120
Eichhornia crassipes	14, 17, 18, 21, 24, 27-29, 31-34	-	-	-
Fishing net	35-50	-	-	-
Ponds	51-75	-	-	-

coming discharge of 70 m^3/s, the mean water level at the exit cross-section of 26.54m, and the flow velocity distribution of three cross-sections (CS-1, CS-2, and CS-3).

The comparison results between the measured and the calculated velocity profiles by the numerical model in this study are shown in Fig. 4. It is found the simulated velocity is in good agreement with the measured velocity, and the numerical model could basically reflect the adjustment effect of vegetation on the floodplain, proving the model has good simulation capabilities. Besides, the simulation result calibrated the Manning coefficient of the main channel of the old course of Fuhe River to 0.021.

APPLICATIONS

To analyze the influence of vegetation on the hydrodynamics of the old course of Fuhe River, this study considered different vegetation development conditions and different combinations of coming discharge from upstream and the

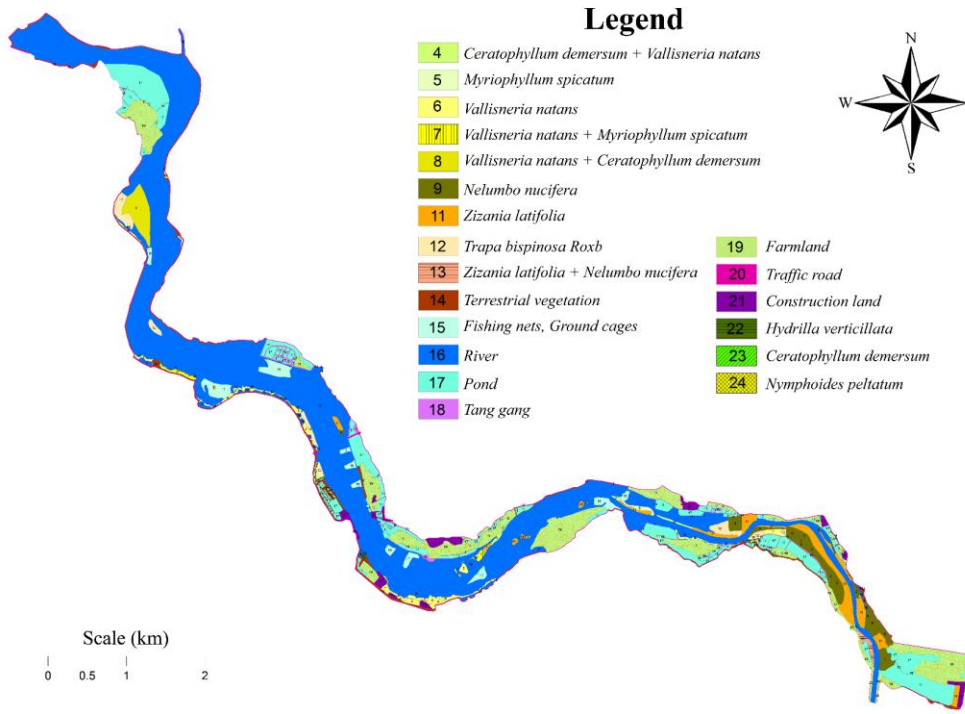

Fig. 2: Vegetation distribution map and land use type of the old course of Fuhe River.

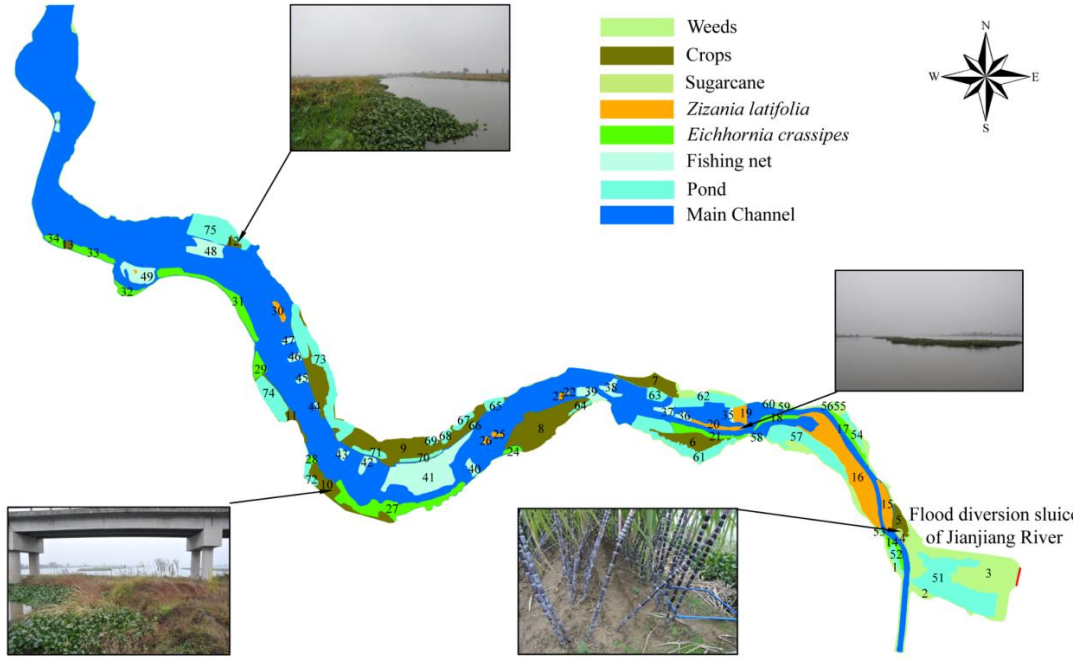

Fig. 3: The simplified map of vegetation distribution and land use types.

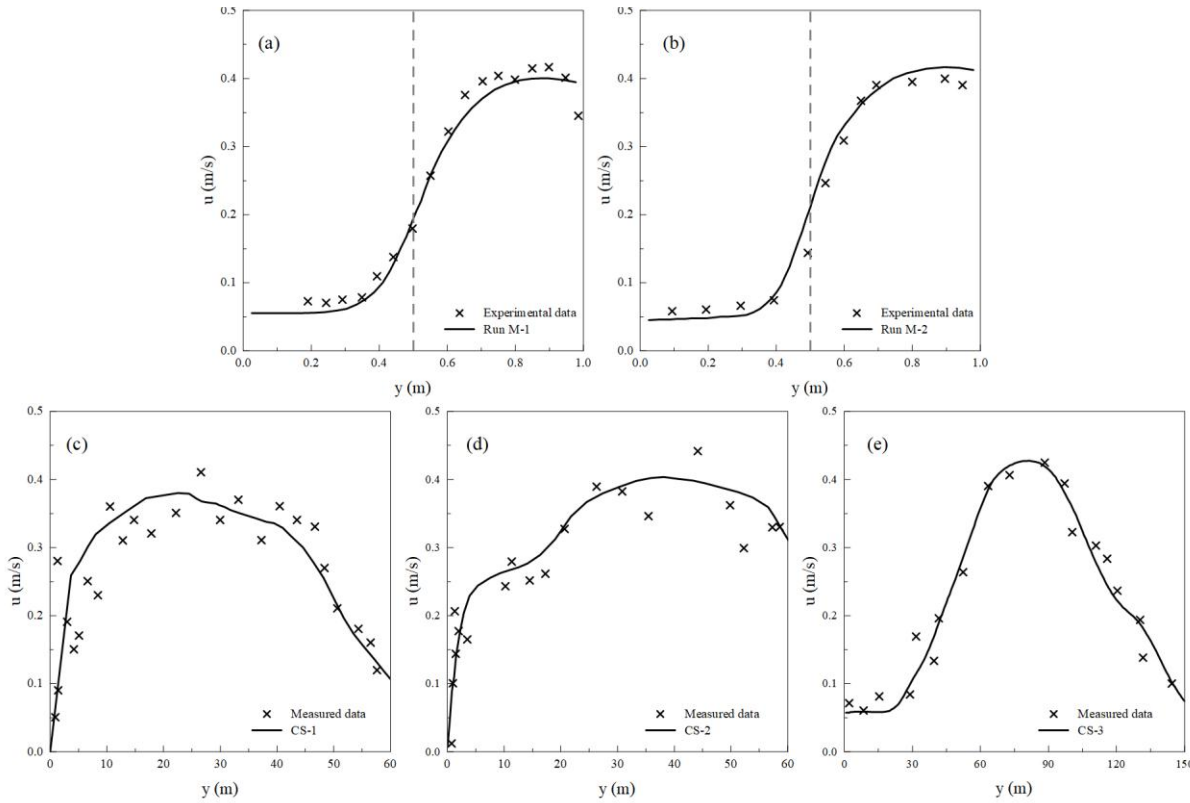

Fig. 4: Comparison results of the simulated and measured velocity.

floodwater discharged from the flood diversion gate. The running conditions simulated by the numerical model are listed in Table 2. The results and analysis would be presented in the following sub-section.

Influence of Vegetation on Hydrodynamics without Flood Diversion

Run A and B listed in Table 2 are the cases without considering the floodwater discharged from the Jianjiang River flood diversion sluice. Based on the vegetation module, the Manning coefficient distribution diagrams of Run A-1 and Run B-1 are shown in Fig. 5. The water depth in the area of *Zizania latifolia* increases with the increase of flow discharge and the resistance of *Zizania latifolia* in the non-submerged state to the water flow has an increasing trend with the value of Manning coefficient ranging from 0.13 to 0.14. According to Fig. 5, the Manning coefficient of the area near the mainstream is greater than that of the central area of *Zizania latifolia* since the water depth is greater in the area near the mainstream, reflecting the roughness of non-submerged vegetation zone increases with water depth rising.

Comparison results in water level and velocity of Run A and Run B are illustrated in Fig. 6 to demonstrate the water-blocking effect of vegetation. The water level of Run A-1 and Run B-1 rises compared to Run A-2and Run B-2, indicating the strong water-blocking effect of *Zizania latifolia*. However, affected by the downstream outlet boundary, the increment of water level is gradually weakened from upstream to downstream. And the largest water level increment exists near the flood diversion gate. The largest water level rises by about 0.09 m in Run A, which is less than the largest rising water level of 0.12 m in Run B. Besides, the mean rising water level of Run B is greater than that of Run A because of the larger incoming discharge. The existence

Table 2: Details of each simulated condition.

Run	$Q[m^3.s^{-1}]$		Water Level at Exist Cross-section [m]	Vegetation Condition
	West Main Canal	Jianjiang River flood diversion sluice		
A-1	70	0	21.54	Existing vegetation
A-2				No vegetation
B-1	110	0	21.80	Existing vegetation
B-2				No vegetation
C-1	110	200	27.50	Existing vegetation
C-2				No vegetation
C-3				Convert farmland to *Zizania latifolia*
C-4				Expand farmland
D-1	110	400	28.00	Existing vegetation
D-2				No vegetation
D-3				Convert farmland to *Zizania latifolia*
D-4				Expand farmland

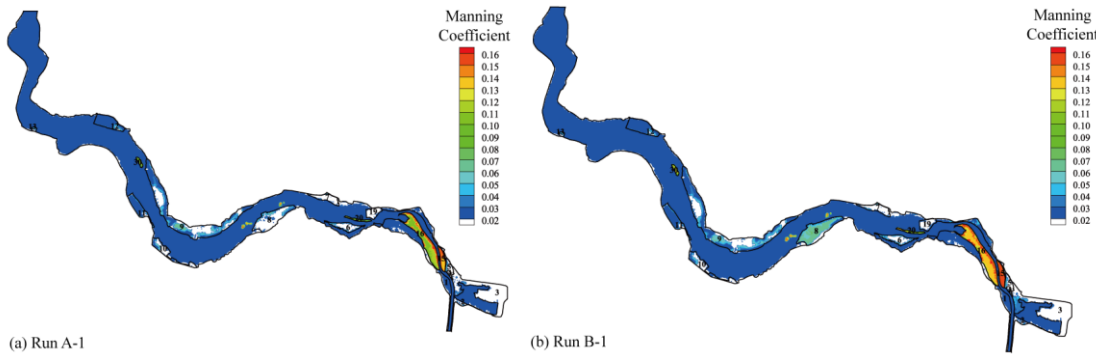

Fig. 5: Manning coefficient diagrams of Run A-1 and Run B-1.

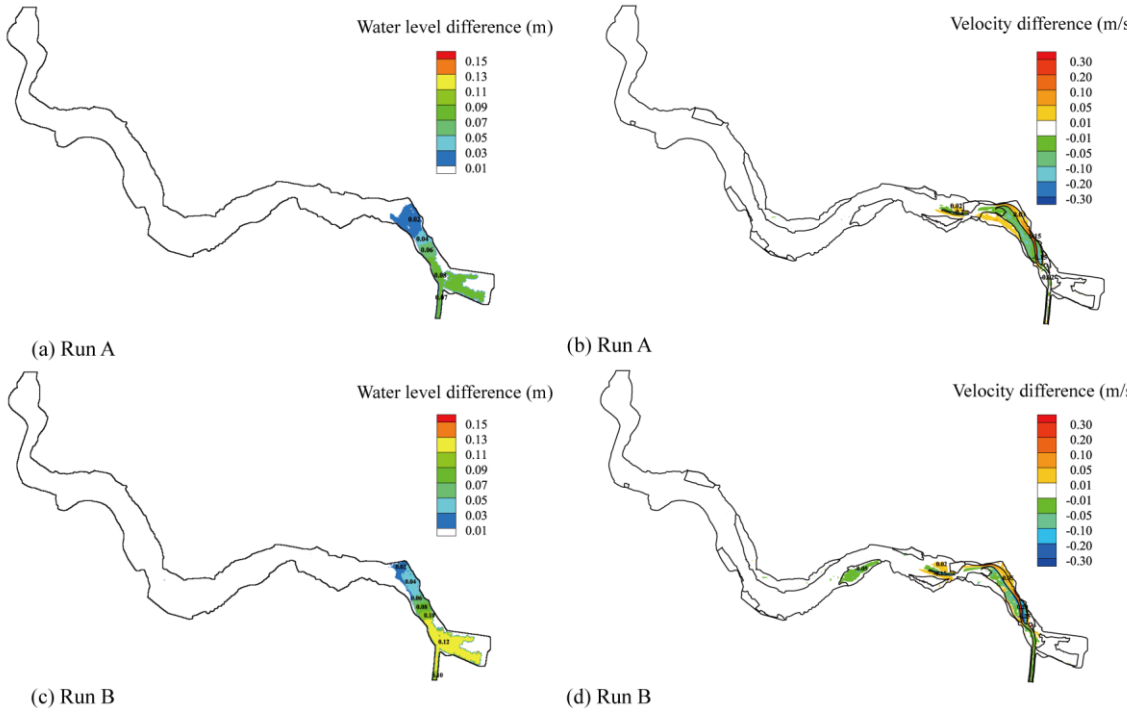

Fig. 6: (a) Water level difference between Run A-1 and A-2; (b) Velocity difference between Run A-1 and A-2; (c) Water level difference between Run B-1 and B-2; (d) Velocity difference between Run B-1 and B-2.

of vegetation causes the velocity in the vegetation area decreases obviously with the largest velocity reduction of 0.2 $m.s^{-1}$ and the velocity in the mainstream increases. And the mean velocity of the whole cross-section decreases because of the rising water level. Similarly, the difference in velocity increases when the incoming discharge gets larger.

Influence of Vegetation on Hydrodynamics Considering Flood Diversion

Considering the floodwater discharged from the flood diversion gate of Jianjiang River, this study analyzed the influence of existing vegetation on the hydrodynamics of the old course of Fuhe River. According to the flood control plan of the Fuhe River basin, the typical flood diversion discharges are $200m^3.s^{-1}$ (Run C) and $400m^3.s^{-1}$ (Run D) respectively.

The Manning coefficient distribution diagrams of Run C-1 and Run D-1 considering the existing vegetation were shown in Fig. 7. It can be seen the roughness of the *Zizania latifolia* area is the largest, followed by the areas of sugarcane, crops, and grass. By studying the roughness induced by *Zizania latifolia*, there are differences in the distribution of roughness in the *Zizania latifolia* area, which is related to the regional topographical fluctuations. Changes in topographical conditions affect the submergence ratio of vegetation, inducing different water-blocking effects. Besides, the Manning coefficient value of vegetation area in Run C-1 is significantly larger than that in Run D-1 by comparing Fig. 7 (a) and (b). Actually, it is related to the relative ratio of water depth to vegetation height. Originally, the water depth is close to vegetation height in Run C-1. However, with the flood diversion discharge increasing to $400m^3.s^{-1}$, the water depth generally spreads over the top of the plant, and the average resistance of vegetation along the water depth shows a downward trend.

Changes in water level difference and velocity difference under the simulated conditions considering flood diversion are similar to that without considering flood diversion. The water-blocking effect of vegetation patches causes water levels rising and the major area of rising water level is mainly near the flood diversion gate of the Jianjiang River. The largest rising water levels under the diversion discharge of $200m^3.s^{-1}$ and $400m^3.s^{-1}$ are 0.17 m and 0.18 m. According to the analysis above, the Manning coefficient decreases since the plants are overwhelmed by water with the discharge increasing to $400m^3.s^{-1}$. However, the mean rising water level under the condition of high flood diversion is larger than that with lower flood diversion. In terms of velocity difference, *Zizania latifolia* located in the upper reaches of the old course

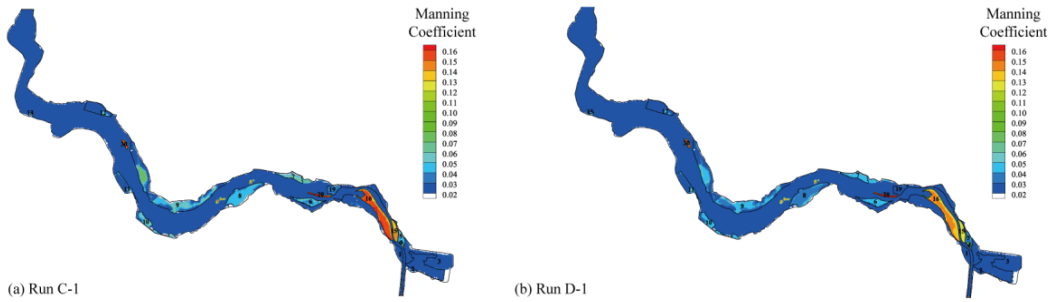

Fig. 7: Manning coefficient diagrams of Run C-1 and Run D-1.

of the Fuhe River has a greater obstruction to river flow. In contrast, other vegetation with low height on floodplains generally appear to be completely submerged under the condition of high flood diversion, and their water-blocking effect is weakened, which is reflected in the smaller decline in the velocity of vegetation area.

To analyze the vegetation influence on velocity distribution, 4 monitoring cross-sections were selected and their locations were presented in Fig. 8 (b) and (d). Changes in velocity distribution are illustrated in Fig. 9. With diversion discharge rising, the velocity of each cross-section generally increases. Besides, it clearly shows a changing trend which is the velocity in the main channel increases while the velocity on the floodplain decreases because of the obstruction of plants on the floodplain.

Considering the ratio of the discharge in the main channel (Q_m) to the discharge on floodplains (Q_f), diversion ratios (Q_m/Q_f) of each cross-section under different flood diversion and vegetation conditions were given in Table 3. The diversion ratio decreases with the increase of flood diversion discharge under the same vegetation condition. As affected by the vegetation, the diversion ratio increases, which means more discharge flows into the main channel, causing the adjustment of velocity distribution.

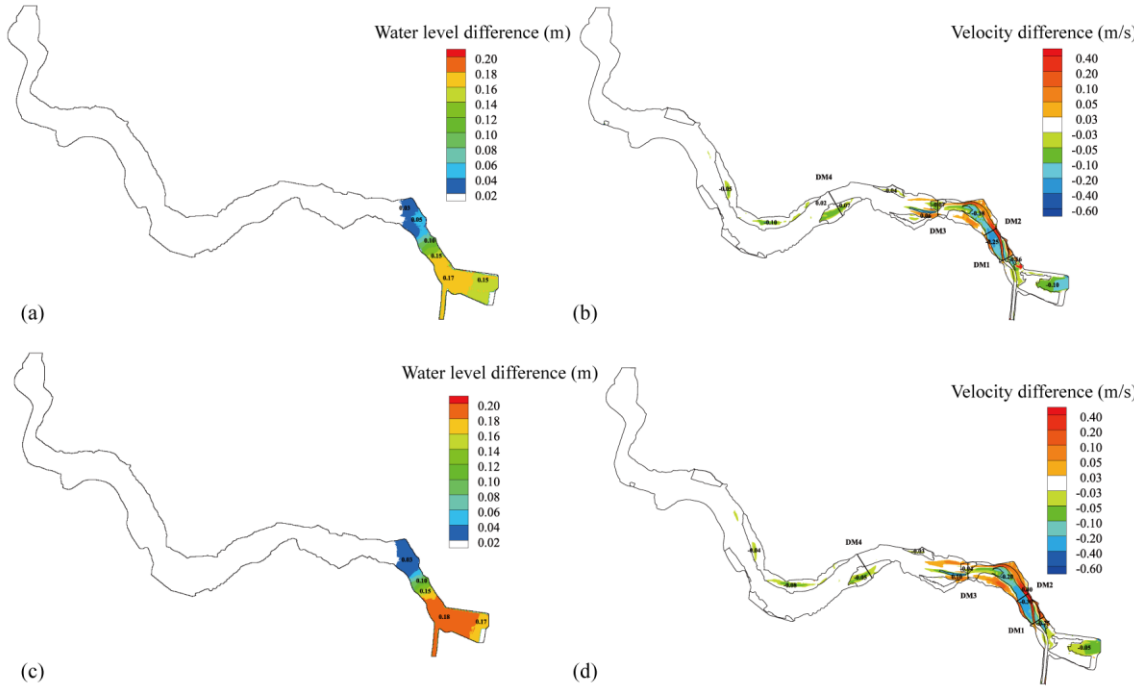

Fig 8: (a) Water level difference between Run C-1 and C-2; (b) Velocity difference between Run C-1 and C-2; (c) Water level difference between Run D-1 and D-2; (d) Velocity difference between Run D-1 and D-2.

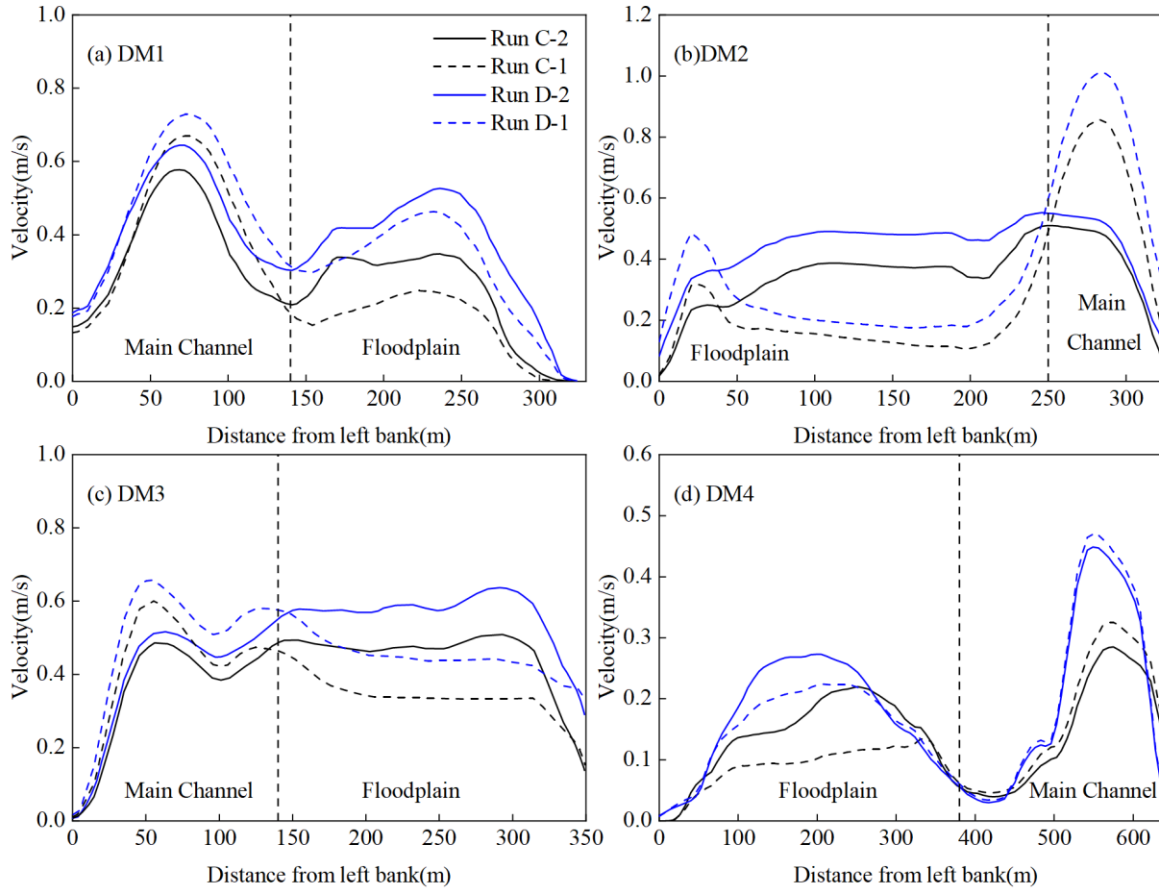

Fig. 9: Velocity distribution of 4 monitoring cross-sections.

Influence of Vegetation on Hydrodynamics Considering Different Vegetation Development Conditions

Social development is accompanied by the contradiction between environmental protection and human survival. On the one hand, to weaken the impact of human activities on the old course of the Fuhe River, the farmland is considered to be converted into the area for growing *Zizania latifolia* which is helpful to promote water quality and ecological environment. On the other hand, with the increase in population, more farmland is needed for growing crops. Hence, to study the influence of changes in land use type on the hydrodynamics in the old course of the Fuhe River, this study considered these two kinds of land use type change illustrated in Fig. 10.

Under the flood diversion discharges of $200m^3.s^{-1}$ and $400m^3.s^{-1}$, the Manning coefficient diagram of each condition was shown in Fig. 11. By comparing Fig. 11 (a) and (b), it could be seen that the Manning coefficient in the areas converted from farmland to growing *Zizania latifolia* has a significant increase with the flood diversion discharge rising. It is because the topography of these areas is relatively high and *Zizania latifolia* is not completely submerged when the flood diversion discharge increases to $400m^3.s^{-1}$. Therefore, with water depth increasing, the emergent *Zizania latifolia* has stronger resistance to water flow. In terms of expanding farmland in the old course of Fuhe River, the Manning coefficient of each farmland area decreases with the flood diversion discharge increasing from $200m^3.s^{-1}$ to $400m^3.s^{-1}$.

Table 3: Diversion ratio of each cross-section under different conditions.

Run	Diversion ratio			
	DM1	DM2	DM3	DM4
C-1	3.70	3.03	2.83	3.92
C-2	3.43	1.67	2.52	3.03
D-1	2.25	2.27	1.43	2.49
D-2	1.08	1.22	1.38	2.14

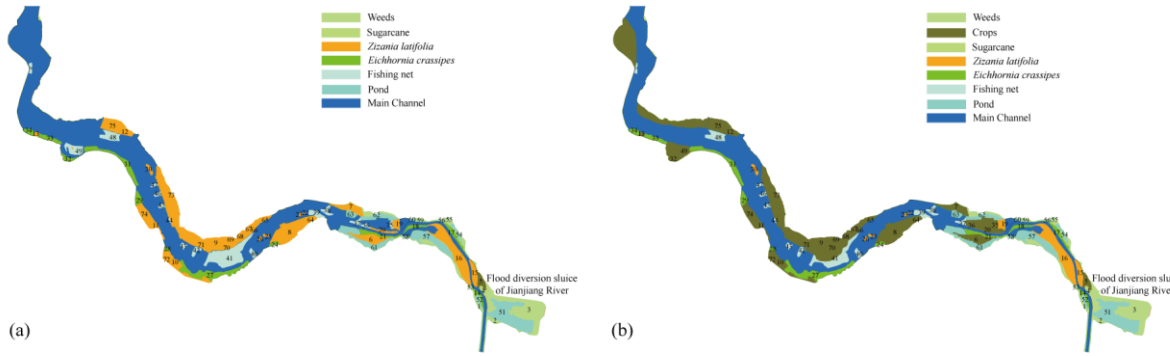

Fig. 10: (a) Convert farmland to *Zizania latifolia*; (b) Expand farmland.

By comparing Run C-3 with Run C-1 and Run D-3 with Run D-1, it was found changes in land use type would cause water levels rising and the significantly affected area is the upstream area of the old course of Fuhe River. Compared with the existing vegetation condition, the largest water level difference is about 0.035m under the flood diversion discharge of $400m^3.s^{-1}$. As for velocity, the affected area is mainly the region where land use type is changed. The decreasing velocity in crop areas indicates that the water-blocking effect of *Zizania latifolia* is stronger than that of crops. Besides, the decrease in velocity of the river bank where farmland is located causes the floodplain velocity on the opposite bank to increase. In terms of expanding farmland, water level and velocity differences are similar to the changing trend illustrated in Fig. 12.

CONCLUSION

This study adopted an equivalent Manning coefficient to establish the mathematical model of the vegetation module.

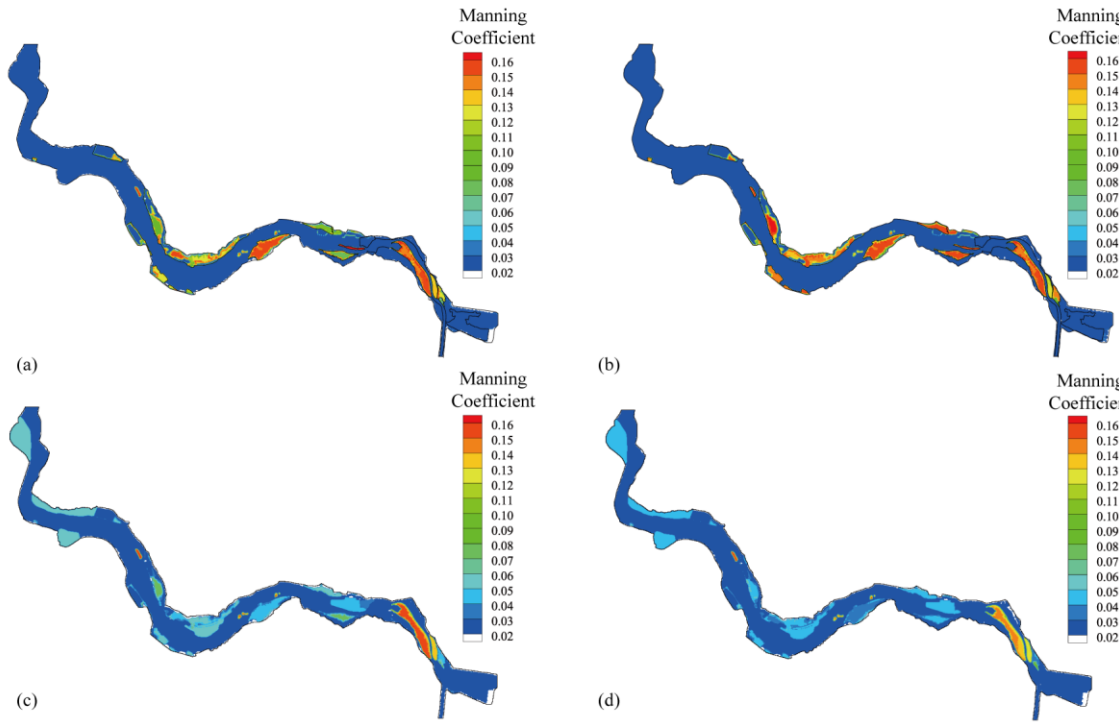

Fig. 11: Manning coefficient diagrams for (a) Run C-3; (b) Run D-3; (c) Run C-4; (d) Run D-4.

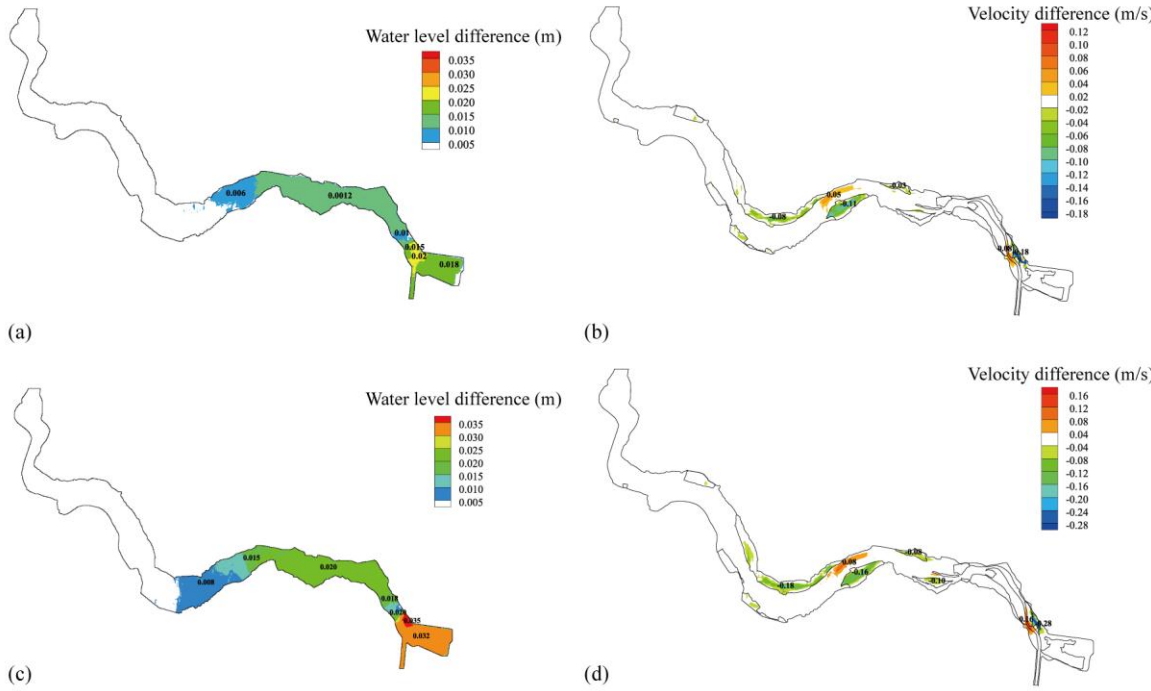

Fig. 12: (a) Water level difference between Run C-3 and C-1; (b) Velocity difference between Run C-3 and C-1; (c) Water level difference between Run D-3 and D-1; (d) Velocity difference between Run D-3 and D-1.

Combined with the hydrodynamic module and field investigation, the influence of vegetation patches on the hydrodynamics in the old course of the Fuhe River was studied by considering various combinations of incoming discharge, flood diversion discharge, and changes in land use type, which could be summarized as below.

(1) The differences in vegetation characteristics (height, diameter, and density) lead to different resistance effects to water flow. Under the same running condition, *Zizania latifolia* has the strongest water-blocking effect followed by sugarcane, crops, and weeds.

(2) The resistance effect of vegetation patches on floodplains causes the local flow velocity to decrease and the water level to rise, which would lead to the adjustment of cross-section velocity. The magnitude of water level difference and velocity difference is related to vegetation resistance and cross-section width.

(3) With the increase in incoming discharge and flood diversion discharge, water level difference and velocity difference induced by vegetation increase.

(4) Converting farmland to *Zizania latifolia* and expanding farmland have similar water-blocking effects. And velocity decreasing in the farmland area on the one side of the river bank would lead to an increase in velocity on the other side of the river bank.

ACKNOWLEDGEMENT

This work was supported by the National Natural Science Foundation of China (Grant No. 51879199) and Major Technology Innovation of Hubei Province (No. 2019ACA154).

REFERENCES

Augustin, L.N., Irish, J.L. and Lynett, P. 2009. Laboratory and numerical studies of wave damping by emergent and near-emergent wetland vegetation. Coast. Eng., 56(3): 332-340.

Bai, F., Yang, Z., Huai, W. and Zheng, C. 2016. A depth-averaged two-dimensional shallow water model to simulate flow-rigid vegetation interactions. Procedia Eng., 154: 482-489.

Cheng, N.S., Wei, M. and Lu, Y. 2020. Critical flow velocity for incipient sediment motion in open channel flow with rigid emergent vegetation. J. Eng. Mech., 146(11): 04020123.

Choi, S.U. and Kang, H. 2004. Reynolds stress modeling of vegetated open-channel flows. J. Hydraul. Res., 42(1): 3-11.

D'ippolito, A., Calomino, F., Alfonsi, G. and Lauria, A. 2021. Flow resistance in the open channel due to vegetation at reach scale: A review. Water, 13(2): 116.

Dijkstra, J.T. and Uittenbogaard, R.E. 2010. Modeling the interaction between flow and highly flexible aquatic vegetation. Water Resour. Res., 46: w12547.

Etminan, V., Ghisalberti, M. and Lowe, R. J. 2018. Predicting bed shear stresses in vegetated channels. Water Resour. Res., 54(11): 9187-9206.

Etminan, V., Lowe, R.J. and Ghisalberti, M. 2017. A new model for predicting the drag exerted by vegetation canopies. Water Resour. Res., 53(4): 3179-3196.

Follett, E. and Nepf, H. 2018. Particle retention in a submerged meadow and its variation near the leading edge. Estuaries and Coasts, 41(3): 724-733.

Ghisalberti, M. and Nepf, H. 2006. The structure of the shear layer flows over rigid and flexible canopies. Environ. Fluid Mech., 6(3): 277-301.

Hou, J., Liang, Q., Simons, F. and Hinkelmann, R. 2013. A stable 2D unstructured shallow flow model for simulations of wetting and drying over rough terrains. Comput. Fluids, 82: 132-147.

Huai, W., Yang, L., Wang, W. J., Guo, Y., Wang, T. and Cheng, Y. 2019. Predicting the vertical low suspended sediment concentration in vegetated flow using a random displacement model. J. Hydrol., 578: 124101.

Huai, W.X., Yang, S.C., Yang, Z.H. and Li, D. 2012. Numerical study of the behavior of the vegetated channel flow. J. Shenzhen Univ. Sci. Eng., 29: 56-60 (in Chinese).

Huang, Z., Yao, Y., Sim, S.Y. and Yao, Y. 2011. Interaction of solitary waves with emergent, rigid vegetation. Ocean Eng., 38(10): 1080-1088.

Li, D., Yang, Z., Zhu, Z., Guo, M., Gao, W. and Sun, Z. 2020. Estimating the distribution of suspended sediment concentration in submerged vegetation flow based on gravitational theory. J. Hydrol., 587: 124921.

Liu, M.Y., Huai, W.X., Yang, Z.H. and Zeng, Y.H. 2020. A genetic programming-based model for a drag coefficient of emergent vegetation in open channel flows. Adv. Water Resour., 140: 103582.

Nepf, H.M. 2012. Flow and transport in regions with aquatic vegetation. Annu. Rev. Fluid Mech., 44: 123-142.

Pasche, E. and Rouvé, G. 1985. Overbank flow with vegetatively roughened flood plains. J. Hydraul. Eng., 111(9): 1262-1278.

Schlichting, H. and Gersten, K. 2017. Boundary-Layer Theory. Springer Berlin Heidelberg, Berlin, Heidelberg.

Sonnenwald, F., Stovin, V. and Guymer, I. 2019. Estimating drag coefficient for arrays of rigid cylinders representing emergent vegetation. J. Hydraul. Res., 57(4): 591-597.

Stone, B.M. and Shen, H.T. 2002. Hydraulic resistance of flow in channels with cylindrical roughness. J. Hydraul. Eng., 128(5): 500-506.

Tinoco, R.O. and Coco, G. 2016. A laboratory study on sediment resuspension within arrays of rigid cylinders. Adv. Water Resour., 92: 1-9.

Toro, E.F., Spruce, M. and Speares, W. 1994. Restoration of the contact surface in the HLL-Riemann solver. Shock Waves, 4(1): 25-34.

Västilä, K. and Järvelä, J. 2018. Characterizing natural riparian vegetation for modeling of flow and suspended sediment transport. J. Soils Sed., 18(10): 3114-3130.

Whittaker, P., Wilson, C.A.M.E. and Aberle, J. 2015. An improved Cauchy number approach for predicting the drag and reconfiguration of flexible vegetation. Adv. Water Resour., 83: 28-35.

Wu, W. and Marsooli, R. 2012. A depth-averaged 2D shallow water model for breaking and non-breaking long waves affected by rigid vegetation. J. Hydraul. Res., 50(6): 558-575.

Yang, J.Q., Kerger, F. and Nepf, H.M. 2015. Estimation of the bed shear stress in vegetated and bare channels with smooth beds. Water Resour. Res., 51(5): 3647-3663.

Yang, J.Q. and Nepf, H.M. 2018. A turbulence-based bed-load transport model for bare and vegetated channels. Geophys. Res. Lett., 45(19): 10428-10436.

Yang, W. and Choi, S. U. 2010. A two-layer approach for depth-limited open-channel flows with submerged vegetation. J. Hydraul. Res., 48(4): 466-475.

Zhao, H., Yan, J., Yuan, S., Liu, J. and Zheng, J. 2019. Effects of submerged vegetation density on turbulent flow characteristics in an open channel. Water, 11(10): 2154.

Zhu, Z., Yang, Z., Bai, F. and An, R. 2018. A new well-balanced reconstruction technique for the numerical simulation of shallow water flows with wet/dry fronts and complex topography. Water, 10(11): 1661.